

# **Challenges in Modelling of Lightning-Induced Delamination; Effect of Temperature-Dependent Interfacial Properties**

---

P. NAGHIPOUR, E. J. PINEDA and S. ARNOLD

## **ABSTRACT**

Lightning is a major cause of damage in laminated composite aerospace structures during flight. Due to the dielectric nature of Carbon fiber reinforced polymers (CFRPs), the high energy induced by lightning strike transforms into extreme, localized surface temperature accompanied with a high-pressure shockwave resulting in extensive damage. It is crucial to develop a numerical tool capable of predicting the damage induced from a lightning strike to supplement extremely expensive lightning experiments. Delamination is one of the most significant failure modes resulting from a lightning strike. It can be extended well beyond the visible damage zone, and requires sophisticated techniques and equipment to detect. A popular technique used to model delamination is the cohesive zone approach. Since the loading induced from a lightning strike event is assumed to consist of extreme localized heating, the cohesive zone formulation should additionally account for temperature effects. However, the sensitivity to this dependency remains unknown. Therefore, the major focus point of this work is to investigate the importance of this dependency via defining various temperature dependency profiles for the cohesive zone properties, and analyzing the corresponding delamination area. Thus, a detailed numerical model consisting of multidirectional composite plies with temperature-dependent cohesive elements in between is subjected to lightning (excessive amount of heat and pressure) and delamination/damage expansion is studied under specified conditions.

---

Paria Naghipour, Ohio Aerospace Institute, 22800 Cedar Point Road  
Cleveland, OH 44142

Evan. J. Pineda, NASA Glenn Research Center MS 49-7, 21000 Brookpark Road,  
Cleveland, OH 44135

Steven M. Arnold, NASA Glenn Research Center MS 49-7, 21000 Brookpark Road,  
Cleveland, OH 44135

## INTRODUCTION

Carbon fiber reinforced polymers (CFRPs) offer significant weight and performance advantages over metals, making them ideal for aerospace applications. However, CFRPs are dielectric (compared to highly conductive metals, such as aluminum); thus when subjected to an electrical impulse (such as a lightning strike) the electricity is not conducted through the CFRP structure. Consequently, the energy from the lightning strike is transformed to thermal energy through resistive super-heating of a highly localized region of the structure near the arc attachment point(s). The extreme surface temperatures induced by the lightning, along with an accompanying high-pressure shockwave (caused by rapid super-heating of the air surrounding the arc) yields extensive visible damage near the arc attachment point, as well as damage away from the arc attachment point that may not be detected through visual inspection. The strike zone (red zone, Figure 1) is the major visible damage zone after a composite panel is hit by a lightning strike. Excessive surface temperatures cause major visible damage such as fiber sublimation and matrix pyrolysis (material recession) and delamination in this area. This strike zone and some area beneath this zone (the blue repair zone in Figure 1) are fully removed and replaced during regular inspection procedures. However, a major area of concern is the residual zone (yellow zone, Figure 1), which is not repaired or replaced after inspection, but might contain highly-damaged areas due to lightning. As a result of a lightning strike, some regions in the residual zone are exposed to very high temperatures (much higher than matrix T<sub>g</sub>), causing major degradation of matrix, fiber, and the interface. Furthermore, exposure of the matrix to such temperatures may increase the susceptibility of the composite to creep deformation during normal service hours. Consequently, delaminations and inelastic matrix deformations are among the major damage mechanism occurring in this zone. However, these sub-critical damages are not easily detected during regular visual inspections, thus they may not be fully included in the repair zone. Accumulation of damage in overlapping residual zones, over multiple lightning strike events, might unexpectedly impact the structural performance of the composite panel significantly. Based on numerical predictions of the extent of the accumulated damage in the residual zone, the repair zone (blue zone, Figure 1) might have to be redefined, so that so that repairs can be completed properly, avoiding any unexpected catastrophic failure.

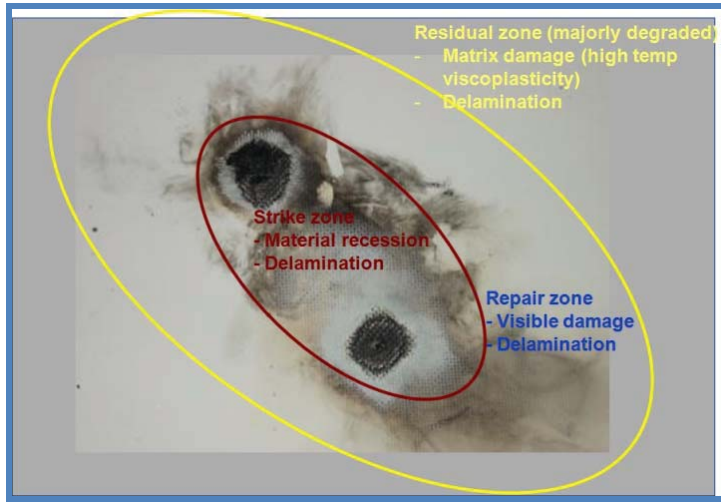


Figure 1. Damage resulting from simulated lightning strike experiment (courtesy of NASA Langley Research Center (LaRC))

Although a predictive numerical tool can provide valuable information on the extent of the lightning-induced delamination damage in the residual zone, developing a competent numerical tool is a very challenging task. Available studies regarding simulated lightning strikes on composite panels are extremely limited [1,6], with almost no attempt to model the damage induced by lightning in CFRPs. Meanwhile, the variation of CFRP properties with high temperatures induced by lightning and the influence of these properties on lightning-induced damage remains largely unknown. Starting with one of the most extensive available experimental studies, a series of simulated lightning strike experiments was conducted by Feraboli and Miller [2] on un-notched and filled-hole carbon/epoxy laminates. The damage area was thoroughly evaluated via ultrasonic scanning, and advanced optical microscopy to gain further understanding of the morphology of damage [2]. Later Kawakami and Feraboli [3] evaluated the effect of repair procedure on the structural performance of wire-mesh protected scarf-repaired carbon/epoxy specimens following a lightning strike. According to the authors [3], a poor repair performs equally or worse than a fully unprotected specimen, and therefore the damage margin (the region to be repaired) has to be defined precisely. Yet, another experimental study by Hirano et al [4] has addressed the evolution of damage in graphite/epoxy composite laminates due to lightning strikes with variations in lightning parameters and specimen size. Ultrasonic testing, sectional observation and micro X-ray inspections were used to assess the damage, which was mainly categorized into fiber damage, resin deterioration, and internal delamination modes. Their results showed that the lightning tests created large delaminations propagating in the shape of a pair of fans starting from the lightning attachment point in each interlayer. In addition to delamination, matrix cracks were also observed, however delamination was emphasized as the dominant failure mode among the others. The experiments in [4] also demonstrated that each damage mode shows correlations with a particular lightning (loading) parameter, nevertheless, variation of specimen geometry has little effect on the damage response. Later Ogasawara et al [5] carried out a finite element (FE) coupled thermal-electrical

analysis of carbon fiber reinforced polymer composites (CFRP) exposed to simulated lightning current, in order to investigate the damage behavior caused by the lightning strike. In their study, the delamination area was estimated to be the same as matrix resin decomposition area (the areas where the temperature was  $> 300$  C), as delamination was assumed to occur because of matrix resin decomposition accompanied by dielectric breakdown of pyrolysis gases. However, no actual continuum delamination modeling was accomplished within the FEM simulation [5].

Based on the mentioned literature [2-5], delamination is the most significant failure mode induced by a lightning strike, which is meanwhile very hard to inspect through regular inspections. When inter-laminar damage (delamination) is the dominant failure mechanism, one recent appealing technique used in capturing delamination is the cohesive zone approach [6-11]. The cohesive zone approach uses interface elements incorporating various traction-separation laws to capture crack initiation and propagation. Since the lightning phenomenon is assumed to be a combination of extreme temperatures and a pressure shockwave leading to extensive inter-laminar damage, the cohesive zone formulation should additionally account for temperature effects. A comprehensive numerical model to predict the amount of lightning-induced delamination in the residual zone is currently not available in the mentioned literature. As the physical phenomenon behind a lightning strike is a very complicated one, a step-by-step methodology shall be followed to devise a general modeling tool for lightning-induced delamination prediction. The first step, which is the major focus of this work, is a systematic sensitivity study to present the effect of temperature-dependent parameters on the delamination progress, utilizing a temperature-dependent cohesive zone formulation.

Following this introduction, constitutive equations of the temperature-dependent cohesive user element are explained concisely. Next, construction of the numerical model, required input parameters, and various patterns of temperature dependency for these parameters are depicted. Numerical simulations of the conducted lightning-induced delamination are presented, and the obtained results are discussed after. Finally, a brief summary and conclusion is presented.

## NUMERICAL MODEL

The numerical FE model consists of individual elastic, transversely isotropic plies and interface elements in between them as shown schematically in Figure 2. As in-ply damage is considered to be less significant based on available experimental evidence [1-5], the only damageable portion is considered to be the interface. The mathematical damage model used for modeling interfacial damage in this work is implemented as a User Element in the FE code ABAQUS by Naghipour et al. [12], and is described briefly in this section.

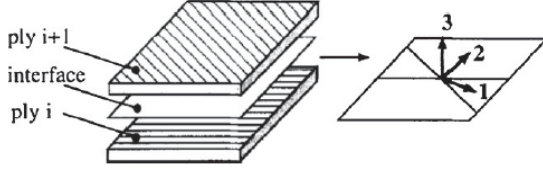


Figure 2. Schematic of lamina and interface elements in the FE model

The pursued mixed-mode cohesive element formulation is based on the constitutive models suggested by Pandolfi and Ortiz [10] and Turon et al. [11] and is further modified to consider the temperature dependency of interface properties. Figure 3 shows the global and local geometries of the three-dimensional 8-node zero-thickness interface element, which are related by the standard isoparametric mapping. Nodes 1-4 represent lower face of the interface and nodes 5-8, which coincide geometrically with nodes 1-4, represent the upper surface. (The zero thickness has been offset for better visualisation).

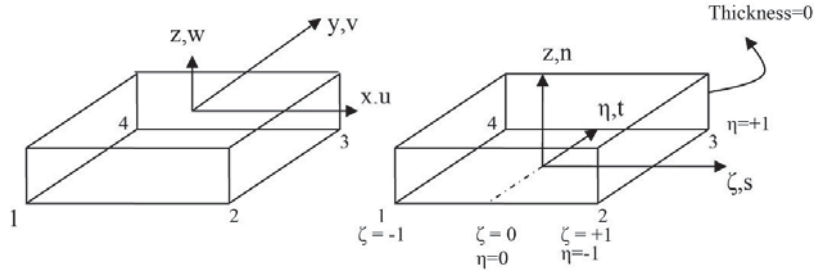


Figure 3. Interface element with (left) global system and (right) local system

With respect to the three-dimensional global coordinate system,  $x$ ,  $y$ ,  $z$ , each node has three degrees of freedom,  $u$ ,  $v$  and  $w$  respectively. Meanwhile, in the local coordinate system the vector of relative displacements between each pair of the corresponding upper and lower nodes of the element is defined as:

$$\begin{bmatrix} \delta_n \\ \delta_s \\ \delta_t \end{bmatrix} = \begin{bmatrix} u_n \\ u_s \\ u_t \end{bmatrix}_{TOP} - \begin{bmatrix} u_n \\ u_s \\ u_t \end{bmatrix}_{BOTTOM} \quad (1)$$

$n$  indicates the opening or normal component and  $s$  and  $t$  indicate the two shear directions, respectively, as shown in Figure 3 (right). The mixed-mode damage formulation is based on constitutive interface tractions ( $\tau_n$ ,  $\tau_s$ ,  $\tau_t$ ) and relative displacements ( $\delta_n$ ,  $\delta_s$ ,  $\delta_t$ ) (Figure 4).

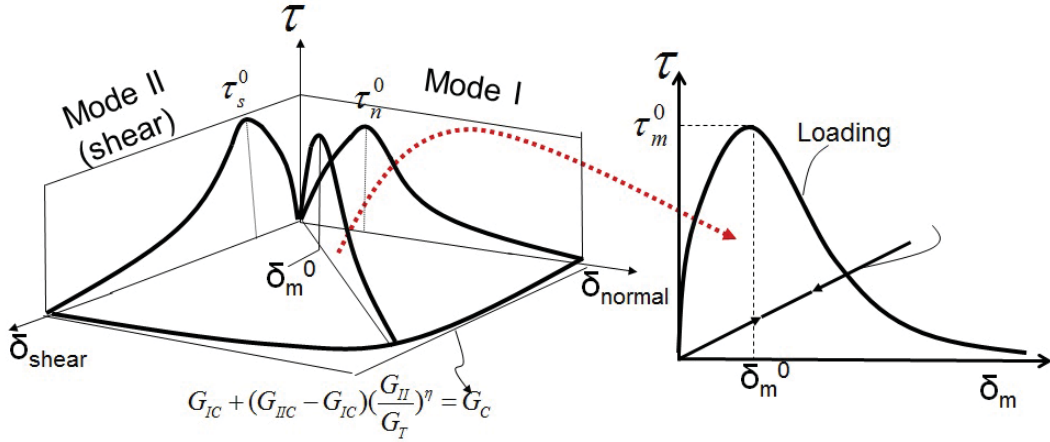


Figure 4. Mixed-mode traction separation law for the cohesive element

Interfacial damage initiates upon satisfaction of the quadratic interfacial traction interaction criterion as shown in Equation (2). The relative displacement corresponding to damage initiation in the mixed-mode plane,  $\bar{\delta}_m^0$  (**Error! Reference source not found.**), is called the mixed mode opening displacement of the fictitious crack tip.

$$\left( \frac{\tau_n}{\tau_n^0(\theta)} \right)^2 + \left( \frac{\tau_s}{\tau_s^0(\theta)} \right)^2 + \left( \frac{\tau_t}{\tau_t^0(\theta)} \right)^2 = 1 \quad (2)$$

$\tau_n^0$ ,  $\tau_s^0$ ,  $\tau_t^0$  are the normal and shear elastic limits of the interface, which are assumed to vary linearly with temperature ( $\Theta$ ). Once the damage is initiated, it starts evolving based on an energy based propagation criterion given by Benzeggagh and Kenane (B-K) [13]:

$$G_{IC}(\theta) + (G_{IIc}(\theta) - G_{IC}(\theta)) \left( \frac{G_{shear}(\theta)}{G_T(\theta)} \right)^\eta = G_c(\theta) \quad (3)$$

$$G_T(\theta) = G_I(\theta) + G_{shear}(\theta)$$

Note, that the form of both the initiation criterion (Equation (2)) and the mixed-mode propagation criterion (Equation (3)) are based upon empirical observations. It is assumed that these forms are adequate for this material system, and testing this hypothesis is beyond the scope of this work. Future experimental studies will be conducted to determine if Equations (2) and (3) can sufficiently fit experimental data under a variety of temperatures and mixed-mode conditions.  $G_{Ic}(\Theta)$  and  $G_{IIc}(\Theta)$  are temperature-dependent fracture toughness values for mode I and mode II that must be determined from fracture experiments conducted under various temperatures. The mixed-mode failure response of the material is described by plotting the total critical fracture toughness  $G_c$  vs. different mode mixities ( $G_{shear}/G_T$ ). Parameter  $\eta$  in Equation (3) maintains the shape of the failure locus in the mixed mode plane, and the most accurate failure criterion is the one matching the material response when plotted in this mixed mode diagram. As the damage evolves based on the mentioned energy-based criterion, an isotropic damage

variable,  $d$ , (Equation 4) degrades the interfacial tractions, till the final separation point ( $\delta_m^f$  in Figure 4) is reached. The damage variable ( $d$ ) degrading the interfacial tractions is calculated at the end of each increment and is compared to determine the initialization and the extent of propagated damage in interface elements.

$$d = \frac{e\tau_m^0 \delta_m^0 \left[ 1 - \left( 1 + \frac{\delta_m^{\max}}{\delta_m^0} \right) e^{-\delta_m^{\max}/\delta_m^0} \right]}{G_c} \quad (4)$$

## FE MODEL DESCRIPTION AND INPUT MATERIAL PROPERTIES

The numerical model was created using the object oriented ABAQUS Scripting Interface (ASI, python) in ABAQUS for further optimization and parametric studies. The laminate is a 500x500 mm square composite panel, made of 10 AS4/PEEK plies (1.4 mm thickness) with a quasi-isotropic stacking sequence and interface elements placed in between laminae. Each lamina is defined using elastic, transversely-isotropic, 8 node, reduced integration, continuum shell elements. The interface elements, implemented as user-defined elements (UEL) in ABAQUS, are placed in between the plies to capture the delamination behaviour.

The material properties for the lamina and the interface (for room temperature) are listed in Table I. Lamina properties, longitudinal and transverse ply stiffness ( $E_{11}$ ,  $E_{22}$ ), Poisson's ratio ( $\nu_{12}$ ), longitudinal and transverse shear modulus ( $G_{12}$ ,  $G_{23}$ ) and their variation with temperature are partially reported in literature [15]. Longitudinal and transverse ply thermal conductivities ( $K_{11}$ ,  $K_{22}$ ,  $K_{33}$ ) are taken from previous literature [4] and assumed to be constant here. However, in order to have a precise numerical model, directional thermal-conductivity data should also be determined as a function of temperature through standardized conductivity experiments. In contrast to ply properties, nothing is available on variation of interfacial properties with temperature in reported literature. Typical interface, which presumably vary with temperature, are normal and shear fracture toughness ( $G_{Ic}$ ,  $G_{IIc}$ ) and corresponding strength values ( $\tau_n^0$ ,  $\tau_s^0$ ). The fracture toughness values at room temperature are measured through available fracture experiments [12].

In order to thoroughly investigate the effect of temperature dependence of the delamination process, the modeling study has been divided into two categories. In the first category, three different temperature dependent profiles for interfacial fracture/ strength values have been assumed. Single mode and mixed mode fracture toughness and strength values ( $G$  and  $\tau$ ) experience a linear reduction to 80%, 40% and 20% of their room temperature values, as the temperature rises from room temperature to 4000 °C. In the second category, mixed mode fracture toughness and strength values experience a linear reduction to 80%, 40% and 20% of their room temperature values, when the temperature rises from room temperature to the glass transition temperature ( $T_g \sim 190$  °C). For temperatures higher than  $T_g$ , the corresponding toughness and strength values are assumed to be close to zero. Note that, assuming different temperature dependent profiles with higher/lower rates of reduction will undoubtedly yield different delamination responses. The profiles here are just initial assumptions, and are not representative of any experimental data. The main focus is to emphasize the significance of temperature-dependent interfacial

properties on lightning-induced delamination response via employing a generic temperature dependence profile. In order to determine precisely the temperature-dependent fracture toughness values, fracture experiments must be conducted under various temperatures, and corresponding fracture loads and crack propagation data must be recorded. However, obtaining fracture data in elevated temperature ranges is a challenging task. Currently, no experimental standards exist for this, and no comprehensive experimental studies have been conducted with definitive success. The results reported in a few studies addressing high temperature fracture testing [16, 17] seem to be inconsistent and need further investigation. Hence, the results of this numerical study can avail as a firm incentive for further research planning on temperature-dependent fracture experiments.

Table I. LAMINA/INTERFACE PARAMETERS AT ROOM TEMPERATURE

Mechanical properties of lamina [15]					
E <sub>11</sub> (MPa)	E <sub>22</sub> (MPa)	v <sub>12</sub>	G <sub>12</sub> (MPa)	G <sub>23</sub> (MPa)	K <sub>11</sub> (W/m/K) K <sub>22</sub> ,= K <sub>33</sub> (W/m/K)
138000	10500	0.3	6300	3500	11.8 0.609
Mechanical properties of interface [12]					
τ <sup>0</sup> <sub>n</sub> (MPa)	τ <sup>0</sup> <sub>s</sub> = τ <sup>0</sup> <sub>t</sub> (MPa)	G <sub>Ic</sub> (mJ/mm <sup>2</sup> )	G <sub>IIc</sub> (mJ/mm <sup>2</sup> )	η	
75	80	0.97	1.72	2.3	

When the panel is subjected to a lightning strike, the transition from the applied electric load into a combination of mechanical (pressure) and thermal (excessive heat) loads is a complicated task. As a result of the resistive joule heating caused by the dielectric nature of the CFRP, the front surface temperature is estimated to be about 3900-4200 °C [4]. However, the numerical simulations presented in Ogasawara (2010) contained a maximum applied temperature of 3000 °C, which is the fiber sublimation temperature. Above these temperature the composite material has completely ablated, and cannot transfer any heat; therefore, a maximum applied temperature of 3000 °C was also used in the simulations presented in this work. Meanwhile a 50 kA strike is supposed to create a high pressure shockwave with an approximate 20-30 MPa pressure in the vicinity of the attachment point [1, 14]. In order to verify the accuracy of the applied loads, the applied temperature and pressure are calibrated so that the backside temperature and displacement correlate with the data from available experimental lightning strikes on unprotected panels. Applied loads are calibrated successfully to match maximum backside temperature (~180 °C) and maximum displacement (~30 mm) of the panel (Figure 5). Accordingly, loading boundary conditions (excessive surface temperatures and a pressure), are applied to the panel in a circular area (radius=10 mm depth= 0.4 mm) in the middle of the panel (Figure 6), and the edges are clamped. The load is applied in a quasi-static manner, as for now there is no possibility to extract the damage variable from an explicit user-defined element in ABAQUS. However, dynamic effects are planned to be included in future studies. As a result of this study number of damaged interface elements is recorded and resulting delamination profiles under the above-mentioned specified boundary conditions are presented.

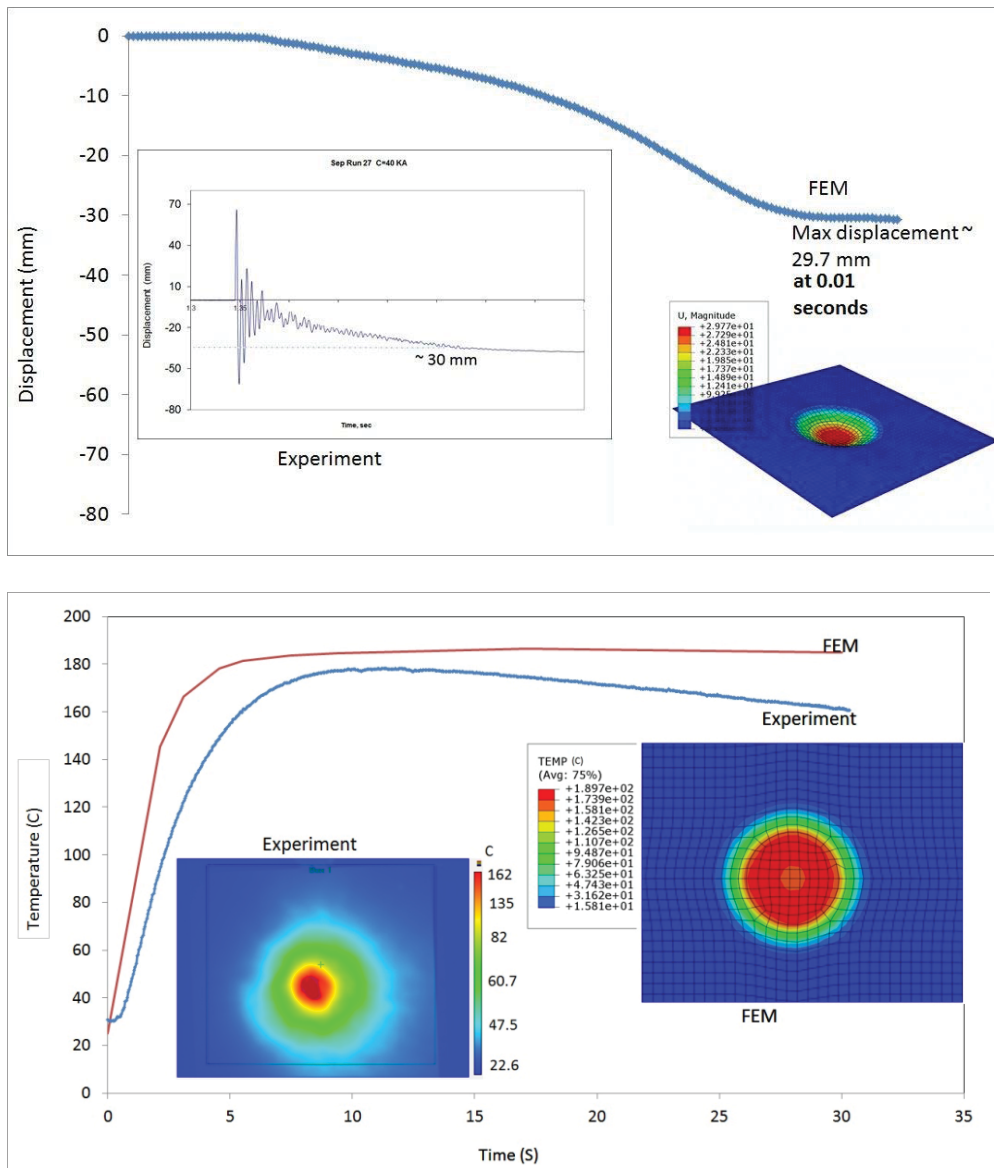


Figure 5. Applied pressure and temperature boundary conditions (calibrated to match the measured backside displacement and temperature of the panel)

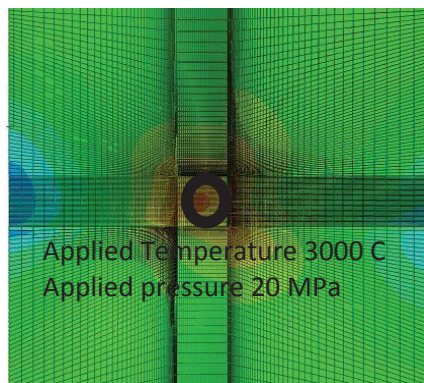


Figure 6. Example FE mesh of the composite plate and applied boundary conditions

## RESULTS AND DISCUSSION

The importance of using accurate temperature-dependent interface properties to predict the lightning induced delaminations is demonstrated in **Error! Reference source not found.**. Three various delamination profiles are compared with each other; first one with no temperature dependency, and the second one with an 80% temperature-dependent linear descent in interface strength and toughness, when the temperature rises to  $4000\text{C}$ , and the third one with an 80% temperature-dependent linear descent in interface strength and toughness, when the temperature rises to  $T_g$ . While we notice a homogenous propagation scheme in the first case, semi fan-shaped delamination propagation is observed for the second case, and we notice a totally random damage profile, distributed over a much wider area in the third case.

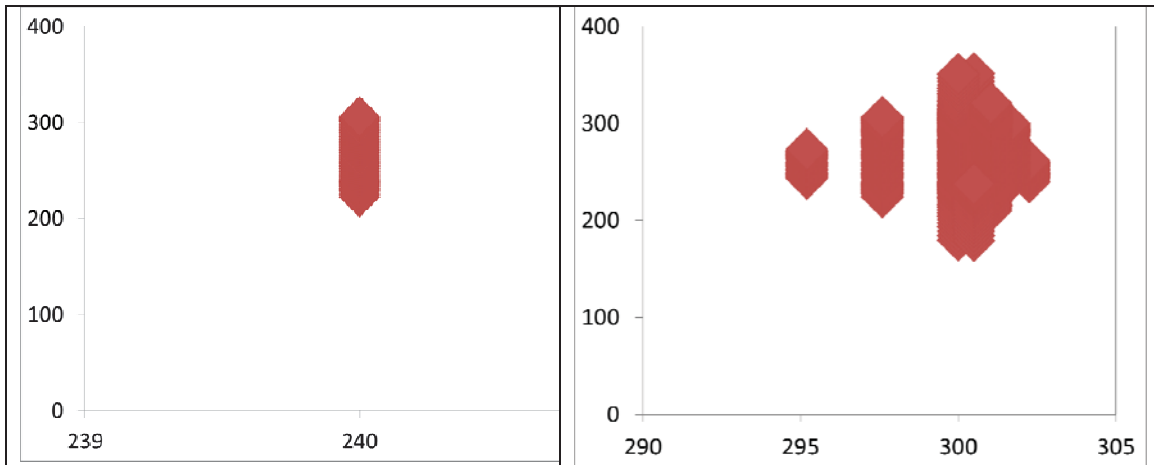


Figure 7a. Delamination profiles: No temperature dependency is assumed (left), 80% linear descent in interfacial properties (strength and toughness) is assumed (right)

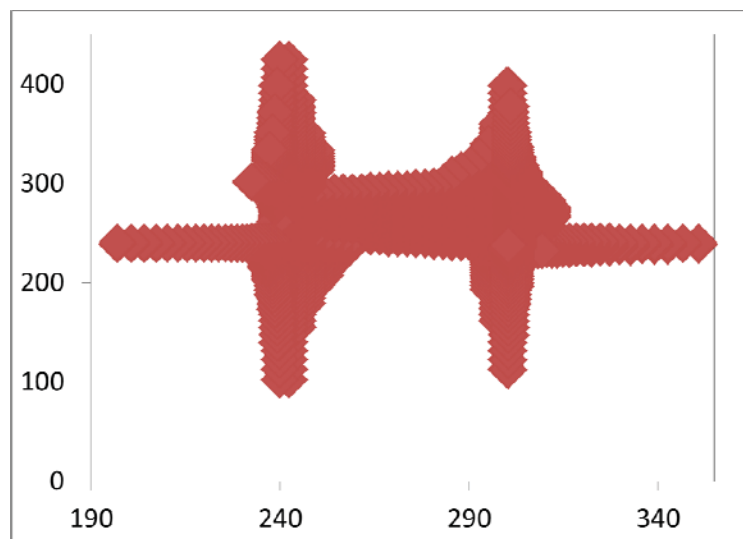


Figure 7b. Delamination profiles: No 80% linear descent in interfacial properties (strength and toughness) is assumed when the temperature rises to  $T_g$

The number of damaged elements in the delamination area does not exhibit a significant rise in the first and second case (Figure 8), however, the delamination profiles are completely different from each other. For the third case, there is a drastic increase in the number of damaged elements as well (Figure 8), which emphasizes the influence of a fast reduction rate of interfacial properties on lightning-induced delamination. Based on observed delamination schemes, the mentioned repair zone (blue zone, **Error! Reference source not found.**) might have to be redefined to avoid any structural failures.

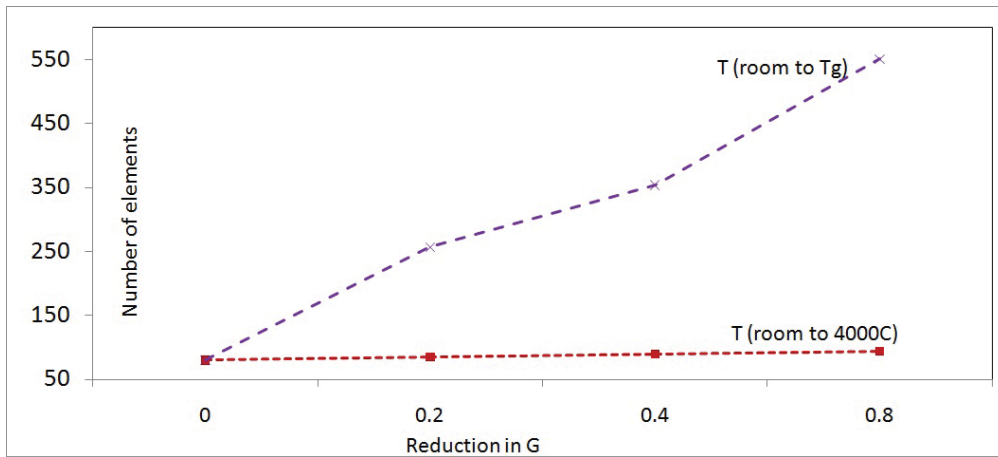


Figure 9. Comparison of number of damaged elements for various reduction rates of fracture toughness in interface elements

## CONCLUSION

A numerical model, consisting of multidirectional plies with temperature-dependent cohesive interface elements in between, was subjected to lightning simulated as a combination of a mechanically applied pressure together with very high thermal gradients. A parametric study was carried out, i.e., corresponding interfacial parameters were varied over a definite temperature range, in order to understand their influence on the predicted lightning damage response. As a basis for comparison, the delamination (number of damaged interfacial elements) was recorded under the specified conditions. It is concluded that, interfacial fracture toughness is the primary parameter controlling lightning-induced delamination propagation. The size of the delamination is strongly dependent on the reduction rate of fracture toughness values with temperature, as higher reduction rates produce a significantly greater number of failed interface elements. It is also observed that the shape of the delamination zone is a significant function of temperature-dependent fracture properties. Based on the shape of the delamination zone, regular repairs might have to be reconsidered to avoid sub-critical failures. Therefore, it can be concluded that measuring the temperature dependence of the fracture toughness is critical in order to predict the delaminated area resulting from a lightning strike. It is worth mentioning that this study is a preliminary study, and further complexities will be built up systematically to capture all the necessary physics and devise a robust lightning-induced damage prediction model.

## REFERENCES

1. Featherston, C.A, M. Eaton, S. L. Evans, K. M. Holford, R. Pullin, and M. Cole. 2010. "Development of a Methodology to Assess Mechanical Impulse Effects Resulting from Lightning Attachment to Lightweight Aircraft Structures", *Applied Mechanics and Material*, 24-25:129-134.
2. Feraboli, P., and M. Miller. 2009. "Damage Resistance and Tolerance of Carbon/Epoxy Composite Coupons Subjected to Simulated Lightning Strike", *Composites: Part A*, 40:954–967.
3. Kawakami, H., and P. Feraboli. 2011. "Lightning Strike Damage Resistance and Tolerance of Scarf-Repaired Mesh-Protected Carbon Fiber Composites", *composites Part A*, 42:1247-1262.
4. Yoshiyasu H., S. Katsumata, Y. Iwahori, and A. Todoroki. 2010. "Artificial Lightning Testing on Graphite/Epoxy Composite Laminate", *composites Part A*, 41:1461-1470.
5. Ogasawara T, Y. Hirano, and A. Yoshimurai. 2010. "Coupled Thermal-Electrical Analysis for Carbon Fiber/Epoxy Composites Exposed to Simulated Lightning Current", *composites Part A*, 41:973-981.
6. Alfano G, and M. A. Crisfield.. 2001. "Finite Element Interface Models for Delamination Analysis of Laminated Composites", *Int J Num Meth Eng*, 50:1701-1736.
7. Allix O, L. Blanchard. 2006. "Mesomodeling of Delamination: Towards Industrial Applications", *Compos Sci and Tech*, 66:731-744.
8. Ladeveze P, L. Guitard, L. Champaney, and X. Aubard. 2000. "Debond Modeling for Multidirectional Composites", *Comp Meth in Appl Mech and Engng*, 183 (1-2):109-122.
9. Serebrinsky S, and M. Ortiz. 2005. "A Hysteretic Cohesive-Law Model of Fatigue-Crack Nucleation", *Scri Mater*, 53:1193-1196.
10. Ortiz M, and A. Pandolfi. 1999. "Finite-Deformation Irreversible Cohesive Elements for Three-Dimensional Crack-Propagation Analysis", *Int J Num Meth Eng*, 44:1267-1282.
11. Turon A, C.G. Davila, P.P. Camanho, and J. Costa. 2007. "An Engineering Solution for Mesh Size Effects in the Simulation Of Delamination using Cohesive Zone Models", *Engng Fract Mech*, 74:1665.
12. Naghipour P, M. Bartsch, and H. Voggenreiter, 2011. "Simulation and Experimental Validation of Mixed Mode Delamination in Multidirectional CF/PEEK Laminates Under Fatigue Loading", *International Journal of Solids and Structures*, 48:1070-1081.
13. Benzeggagh M.L, and M. Kenane. 1996. "Measurement of Mixed-Mode Delamination Fracture Toughness of Unidirectional Glass/Epoxy Composites With Mixed Mode Bending Apparatus", *Compos Sci Tech*, 56:439-449.
14. Hill R.D. 1971. "Channel Heating in return Strike Lightning", *Journal of Geophysical Research*, 76 (NO. 3).
15. Kohlgruber D. 1997. Internal report: "Mechanical in-plane failure properties of PEEK/AS4. Source: CYTEC /DLR. Institute of Structures and Design, German Aerospace center -DLR. Stuttgart.
16. Reeder J.R. 2002. "Prediction of Long-Term Strength of Thermoplastic Composites Using Time-Temperature Superposition", NASA/TM-2002-211781.
17. Johnson, W. S., and P. D. Mangaligiri, "Influence of the Resin on Interlaminar Mixed-Mode Fracture," NASA/TM-87571, 1985.